Electronic Supplementary Material (ESI) for Journal of Materials Chemistry A.

Supporting Information

Synthesis of High-Purity Li_2S Nanocrystals via Metathesis for Solid-State Electrolyte Applications

William H. Smith,[a] Saeed Ahmadi Vaselabadi,[a] Colin A. Wolden[a]*

[a]*Department of Chemical and Biological Engineering, Colorado School of Mines, Golden, CO United States*

**Email: cwolden@mines.edu*

Supplemental Results and Discussion

While most attention has been paid to reducing the presence of oxygenated impurities in the Li_2S-m, relatively little has been focused on the NaCl that is retained due to nonzero solubility in EtOH. It is expected that due to the strong bond enthalpy of NaCl, it would be fairly inert during cell operation, though it may contribute to cell resistance due to its insulating nature. The separation efficiency of Li_2S and NaCl in EtOH is dependent on the relative solubility of the two species, with an expected concentration of ~1.5 wt% NaCl in Li_2S at the concentrations employed here. Others have suggested reacting Na_2S with a stoichiometric excess of LiCl, to result in unreacted LiCl that suppresses NaCl dissolution via the common-ion effect.[20] The residual LiCl can be removed by solvent washing or used as a Cl source in the synthesis of SSEs such as Li_6PS_5Cl. However, in our case unreacted LiCl preferentially formed Li_3OCl without purification. We suggest that the common-ion effect may be more effective when combined with one of the purification strategies presented here.

We also explored the option of utilizing a longer chain alcohol – 1-propanol (PrOH) – because of its lower NaCl solubility relative to Li_2S, which could theoretically reduce the NaCl concentration to ~0.5 wt%. We demonstrate that Li_2S-c and Li_2S-m recovered from PrOH both result in oxygenated impurities when annealed at 200 °C. However, H_2S-drying at 80 °C seems effective at suppressing these impurities as shown in XRD and FTIR. (Fig. S8-a,b) The microstructure of the H_2S-dried material recovered from PrOH appears similar to the EtOH-derived material, though with a higher degree of agglomeration. (Fig. S8-c) The relative concentrations of Na and Cl in the EtOH and PrOH materials were measured with EDAX. However, both samples showed nearly identical EDAX peak intensities (Fig. S8-d), suggesting that the actual solubility of NaCl is affected by the presence of co-solutes like Li_2S, or that Na and Cl is contributed from alternate sources, such as Na_2S or LiCl. Further work is needed to both reliably quantify and reduce the NaCl content of the Li_2S.

Finally, in a previous study we explored the use of low-purity dehydrated Na_2S (Na_2S-d) as the precursor for Li_2S formation.[19] The resulting Li_2S exhibited higher concentrations of Li_2CO_3, and Li_6PS_5Cl argyrodites fabricated from Na_2S-d-derived Li_2S contained crystalline Na_2S. However, the ionic conductivity of these samples was generally higher even than materials derived from battery-grade Li_2S. Figure S9 displays XRD and FTIR of Li_2S synthesized from Na_2S-d (5% excess) and LiCl in EtOH with annealing at 200 °C under Ar or at 80 °C under 10% H_2S, demonstrating that the H_2S drying may be applicable to purification even when lower purity Na_2S is employed. Such a process could represent the simplest and most economical route from Na_2S to Li_2S, since Na_2S purification steps such as hydrogen reduction or recrystallization could be avoided.

Supplemental Figures

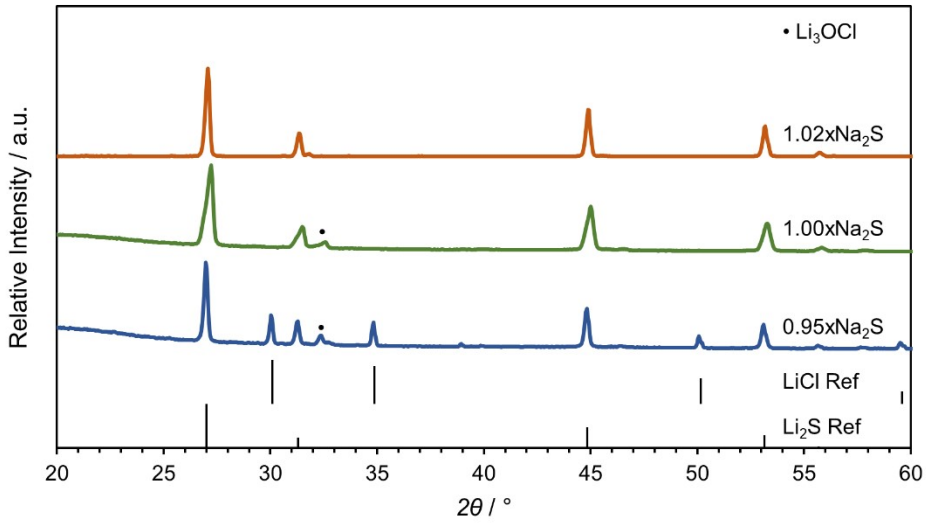

Figure S1. XRD of Li_2S dried at 250/300 °C for 12 h each after recovery from LiCl-Na_2S reactions in ethanol by solvent evaporation. Reactions were conducted by adding varying fractions of stoichiometric Na_2S to a LiCl-EtOH precursor solution and stirring for 24 h.

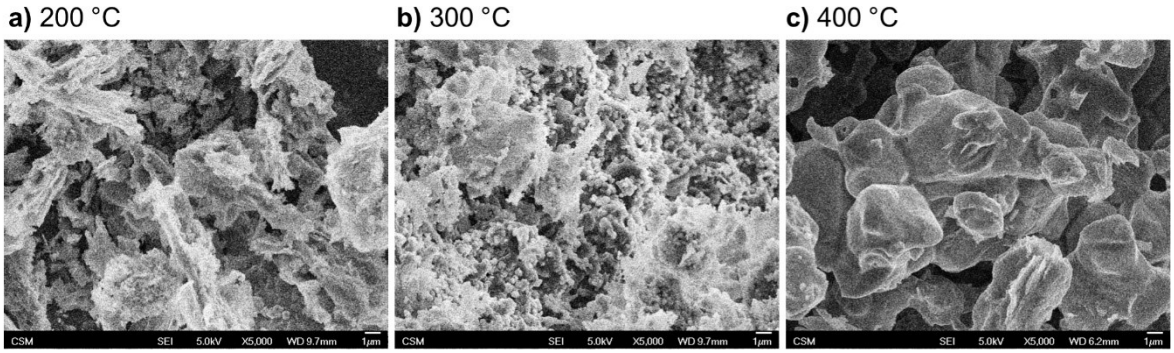

Figure S2. SEM images of Li_2S-m annealed at different temperatures under Ar.

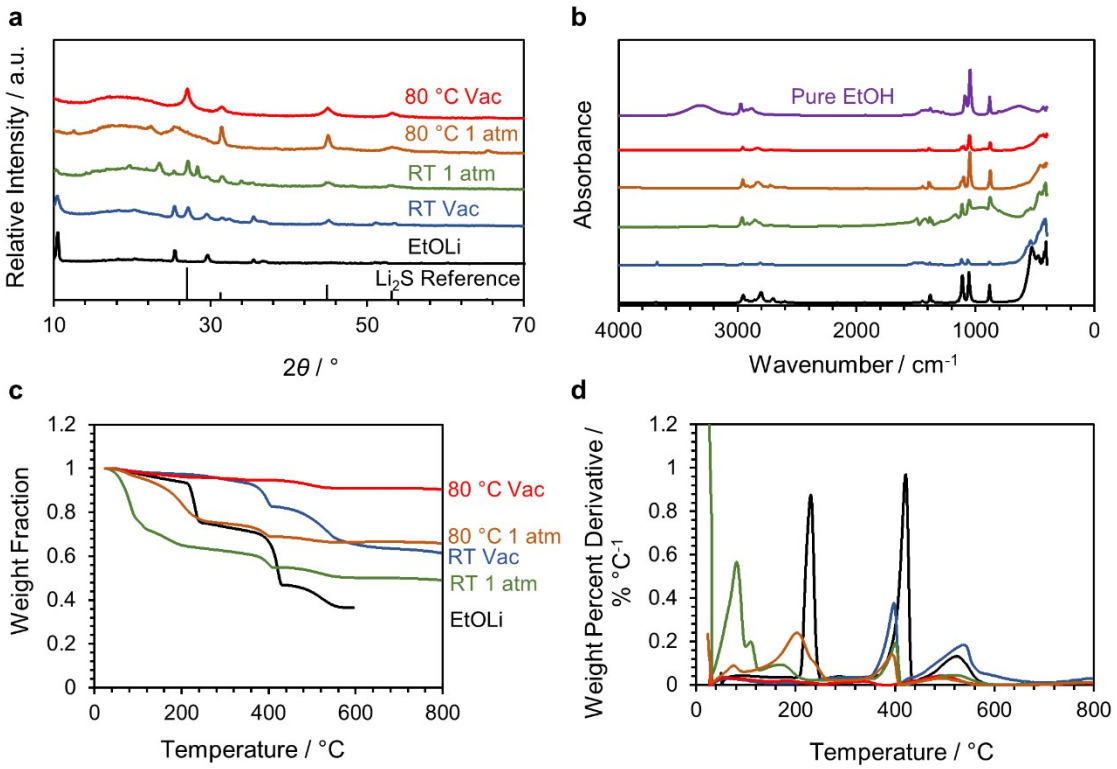

Figure S3. a) XRD, b) FTIR, c) TGA, and d) derivative of TGA of Li_2S-c recovered from EtOH under different drying conditions compared to EtOLi.

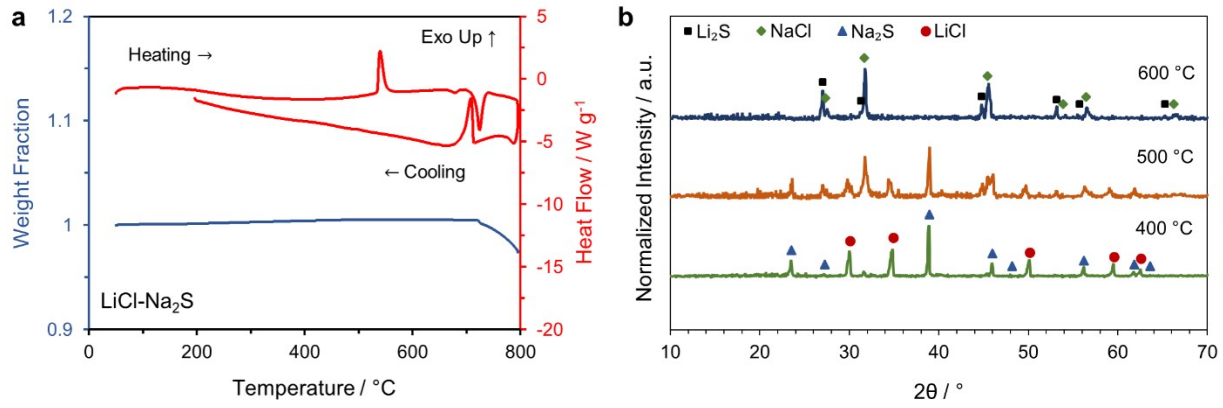

Figure S4. a) DSC/TGA of a mixture of Na_2S and LiCl. b) XRD of a mixture of Na_2S and LiCl after heating to different temperatures for 2 h under Ar.

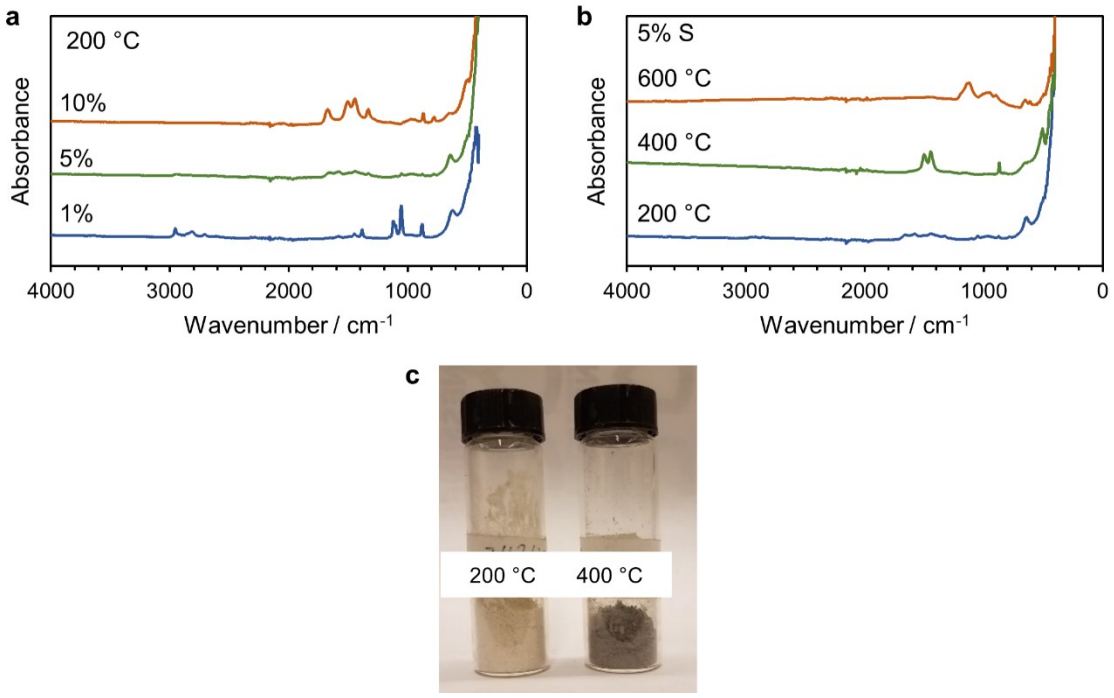

Figure S5. a) FTIR of Li_2S-m annealed at 200 °C with different sulfur loadings, and b) with 5% sulfur loading at different temperatures. c) Optical images of Li_2S-m at 5% sulfur loading annealed at different temperatures.

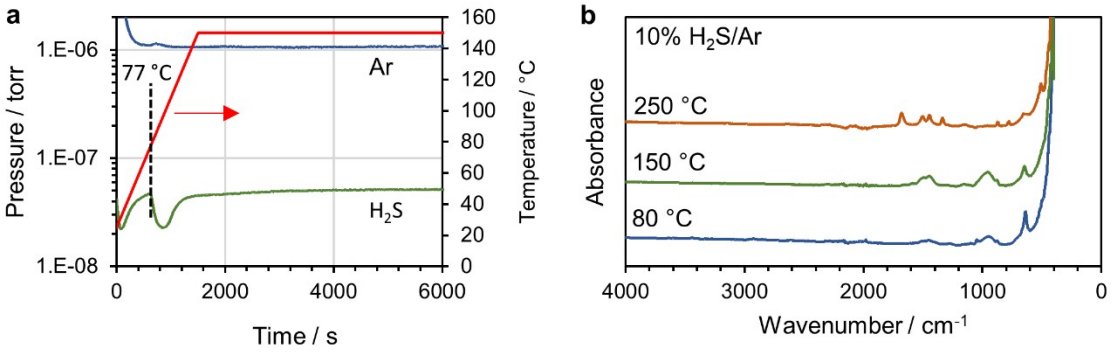

Figure S6. a) On-line mass spectrometry of effluent from Li_2S-m under 10% H_2S in Ar during heating. Ar (m/z = 40) and H_2S (m/z = 34) b) FTIR of Li_2S-m heated to different temperatures under 10% H_2S in Ar.

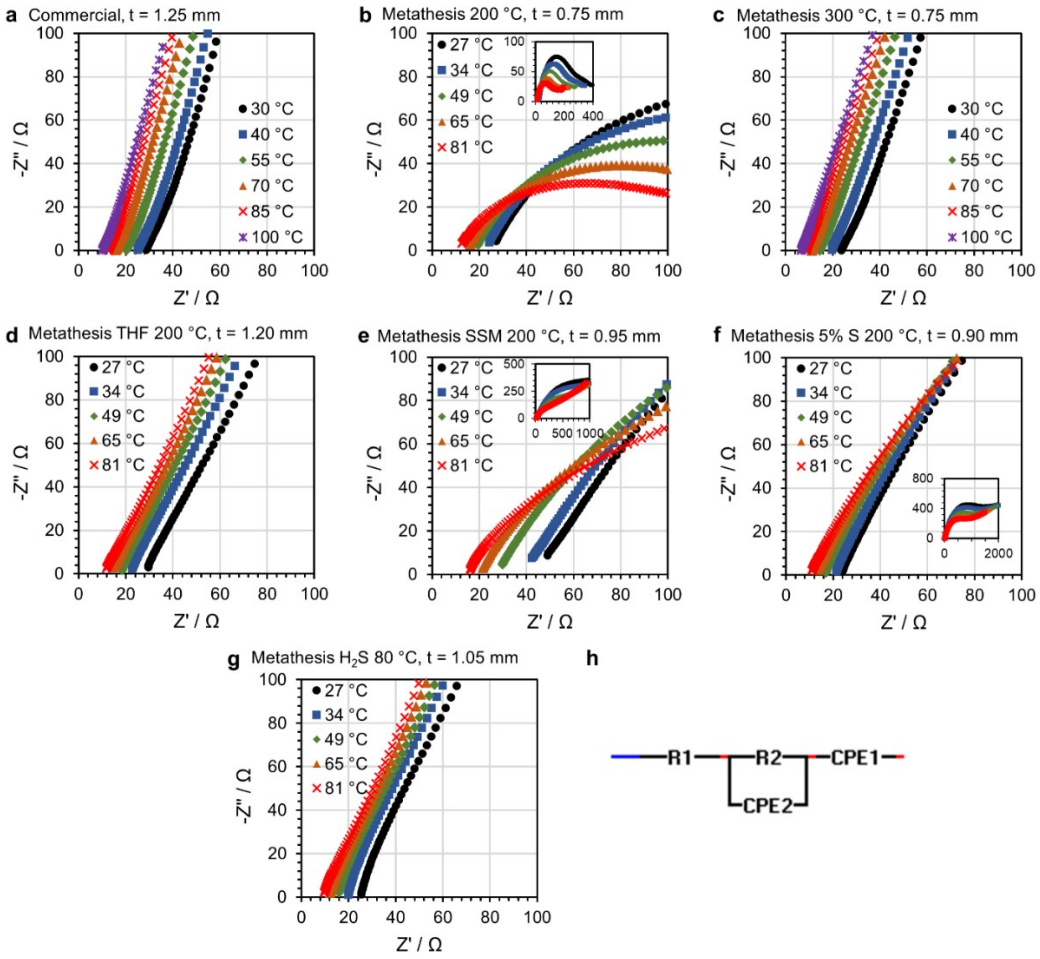

Figure S7. a-g) Nyquist plots at different temperatures of Li_6PS_5Cl argyrodites fabricated from different Li_2S samples. Insets display fuller scale to showcase semicircles when observed. h) Equivalent circuit used for fitting data in e and f. For fitting data in b, an additional RQ element was added in series.

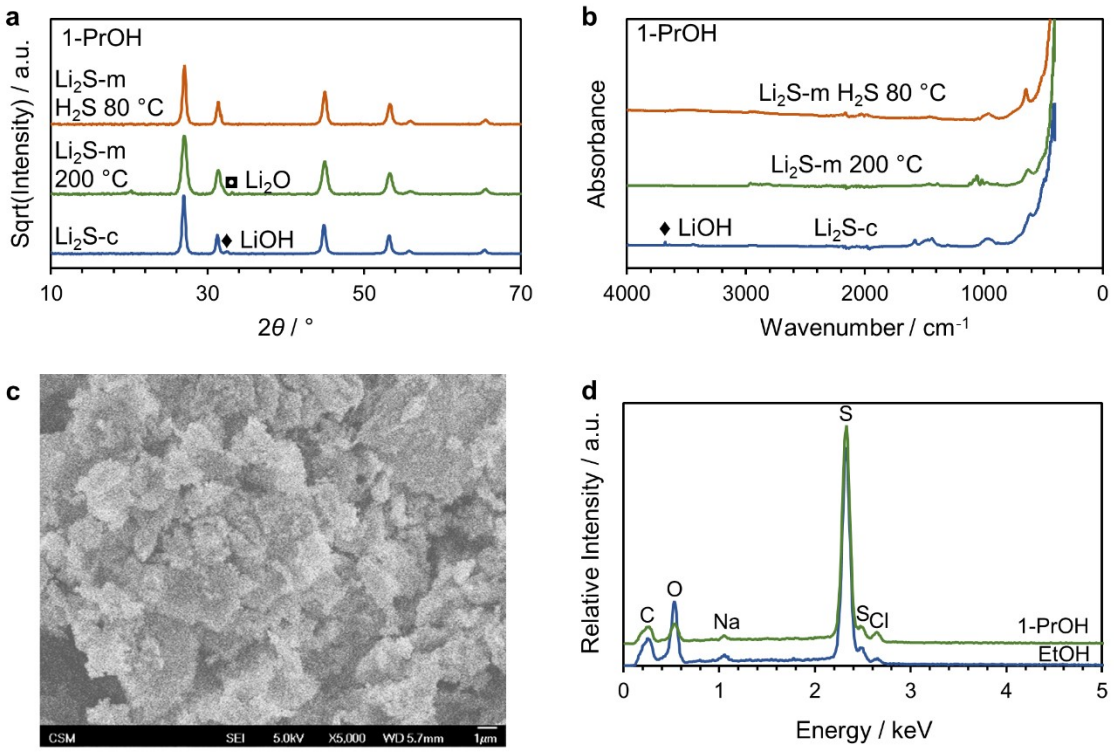

Figure S8. a) XRD and b) FTIR of Li_2S-c and Li_2S-m recovered from PrOH. c) SEM image of Li_2S-m recovered from PrOH with drying under H_2S at 80 °C. d) EDAX spectra of Li_2S-m recovered from EtOH or PrOH with drying under H_2S at 80 °C.

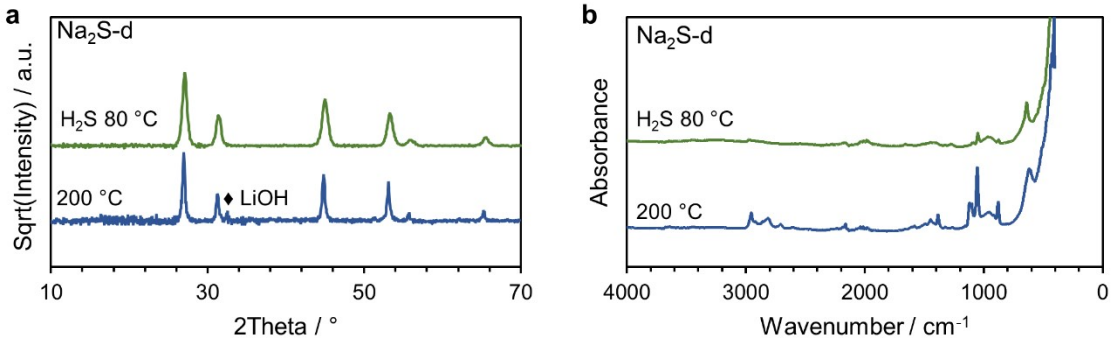

Figure S9. a) XRD and b) FTIR of Li_2S-m derived from Na_2S-d with annealing at 200 °C under Ar or drying at 80 °C under 10% H_2S in Ar.